



HAL
open science

Impact and compression after impact experimental study of a composite laminate with a cork thermal shield

Sandrine Petit, Christophe Bouvet, Alain Bergerot, Jean-Jacques Barrau

► To cite this version:

Sandrine Petit, Christophe Bouvet, Alain Bergerot, Jean-Jacques Barrau. Impact and compression after impact experimental study of a composite laminate with a cork thermal shield. *Composites Science and Technology*, 2009, 67 (15-16), pp.3286. 10.1016/j.compscitech.2007.03.032 . hal-00509042

HAL Id: hal-00509042

<https://hal.science/hal-00509042>

Submitted on 10 Aug 2010

HAL is a multi-disciplinary open access archive for the deposit and dissemination of scientific research documents, whether they are published or not. The documents may come from teaching and research institutions in France or abroad, or from public or private research centers.

L'archive ouverte pluridisciplinaire **HAL**, est destinée au dépôt et à la diffusion de documents scientifiques de niveau recherche, publiés ou non, émanant des établissements d'enseignement et de recherche français ou étrangers, des laboratoires publics ou privés.

Accepted Manuscript

Impact and compression after impact experimental study of a composite laminate with a cork thermal shield

Sandrine Petit, Christophe Bouvet, Alain Bergerot, Jean-Jacques Barrau

PII: S0266-3538(07)00142-X
DOI: [10.1016/j.compscitech.2007.03.032](https://doi.org/10.1016/j.compscitech.2007.03.032)
Reference: CSTE 3653

To appear in: *Composites Science and Technology*

Received Date: 7 November 2006
Revised Date: 21 March 2007
Accepted Date: 23 March 2007

Please cite this article as: Petit, S., Bouvet, C., Bergerot, A., Barrau, J-J., Impact and compression after impact experimental study of a composite laminate with a cork thermal shield, *Composites Science and Technology* (2007), doi: [10.1016/j.compscitech.2007.03.032](https://doi.org/10.1016/j.compscitech.2007.03.032)

This is a PDF file of an unedited manuscript that has been accepted for publication. As a service to our customers we are providing this early version of the manuscript. The manuscript will undergo copyediting, typesetting, and review of the resulting proof before it is published in its final form. Please note that during the production process errors may be discovered which could affect the content, and all legal disclaimers that apply to the journal pertain.



Impact and compression after impact experimental study of a composite laminate with a cork thermal shield

Sandrine Petit*, Christophe Bouvet**, Alain Bergerot*** and Jean-Jacques Barrau**

* LMS, IPPT PAN, École Nationale Supérieure de l'Aéronautique et de l'Espace
10, avenue E. Belin - 31055 Toulouse Cedex 4 - FRANCE

** LGMT, IGM, Université Paul Sabatier
118, route de Narbonne - 31062 Toulouse Cedex 04 - FRANCE

*** EADS Space Transportation
rue du général Niox - 33160 Saint Médard en Jalles - FRANCE

Authors to whom correspondence must be sent :

C. Bouvet

Université Paul Sabatier

Filière Génie Mécanique, Bât. 3PN

118, route de Narbonne – 31062 Toulouse cedex 04 – France

Tel : 33-(0)5-61-55-84-26

Fax : 33-(0)5-61-55-81-78

Email : bouvet@lgmt.ups-tlse.fr

Abstract :

The aim of this paper is to present an experimental study of impact and compression after impact (CAI) tests performed on composite laminate covered with a cork thermal shield (TS) intended for launchers fairing. Drop weight impact tests have been performed on composite laminate sheets with and without TS in order to study its effect on the impact damage. The results show the TS is a good mechanical protection towards impact as well as a good impact revealing material. Nevertheless, totally different damage morphology is obtained during the impact test with or without TS, and in particular at high impact energy, the delaminated area is larger with TS. Afterwards, CAI tests have been performed in order to evaluate the TS effect on the residual strength. The TS appears to increase the residual strength for a same impact energy, but at the same time, it presents a decrease in residual strength before observing delamination. In fact, during the impact tests with TS, invisible fibres' breakages appear before delamination damage contrary to the impacts on the unshielded sheets.

Keywords : Impact behaviour (B), Damage tolerance (C), Delamination (C), Residual stress (C)

I) Introduction

Composite materials have been increasingly introduced in airframe and spatial applications in the last decade because of their interesting characteristics, like their low specific weight, enhanced mechanical strength, high stiffness... Nevertheless, during the structure's life, damage induced in these materials by impacts of minor and major objects like hail stones, runway debris or dropping tools can drastically decrease the structure's life. Consequently, it is essential to define a damage tolerance demonstration as soon as a new project begins. Damage tolerance is intended to ensure that, with serious fatigue, or accidental damage occurring within the operational life of the airplane, the remaining structure can withstand reasonable loads without failure or excessive structural deformation until the damage is detected. The accidental damage is characterised by its visual detectability (cf. figure 1) and compared to the so called barely visible impact damage (BVID) which is a very important concept in relation to the damage tolerance and fatigue evaluation (JAR25.571).

The aviation requirements, e.g. JAR25.571, state that the effect of damage on the strength of the structure must be analysed and controlled through the application of a proper design philosophy and proper maintenance and repair.

The damage tolerance philosophy was introduced at the end of 1978 for aircraft structures [1, 2]. But in the military and spatial launchers' fields, the damage tolerance concept has been introduced recently.

This study presents the characterisation works performed on laminates used for civil and military launchers' fairing considering damage tolerance demonstration. The accidental damage are realized with a drop weight system which allow to perform low velocity impact tests [3, 4]. Afterwards residual strength is classically evaluated thanks to compression after impact (CAI) tests [5, 6, 7, 8].

The impact's problem on laminated structures has been a subject of intense research efforts [9, 10, 11, 12...], but this work's feature is the cork thermal shield (TS) glued on composite panels and its effect on the damage tolerance demonstration. This TS is made of natural cork pellets agglomerated by impregnation and polymerisation of a phenolic nitrile resin and is glued on civil and military launchers' fairing as thermal protection system. But during impact tests, this thermal protection modifies the structure behaviour and causes unusual impact damage.

This original damage morphology influences the structure behaviour during the CAI test and modifies the residual strength compared with unshielded panels [13, 14].

These tests could allow analysing and improving numerical models under impact and CAI on an unusual case which product different results than the classical ones on unshielded panels.

II) Impact experimental investigation

II-1) Materials and specimens

Two composite materials, with carbon fibres and epoxy matrix, are tested in this investigation : a high modulus (HM) unidirectional composite, often used in spatial structures and, a well known aeronautical material, a high strength (HS) unidirectional composite T300/914 are used. The names of HM and HS are used in regards, respectively, with the high modulus ($E_1^t = 230$ GPa in the longitudinal direction) and with the high failure strain ($\epsilon_1^t = 11540 \cdot 10^{-6}$ in the longitudinal direction) in the fibres direction. The complete mechanics' characteristics of these materials, determined by experimental tests, are given table 1.

E_1^t , E_1^c are the Young modulus, respectively in tension and compression in the fibres direction (1), E_2 the Young modulus in the transverse direction (2), σ_1^t , σ_1^c the failure stresses, respectively in tension and compression in the fibres direction, σ_2^t , σ_2^c the failure stresses, respectively in tension and compression in the transverse direction, τ_{12} the failure shear stress in the 1-2 plane, ϵ_1^t , ϵ_1^c the failure strains, respectively in tension and compression in the fibres direction determined by the ratio between the failure stress and the Young modulus and ν_{12} the poisson's ratio in the 1-2 plane.

HM rectangular panels of $150 \times 100 \times 3.78$ mm³ are manufactured with 18 unidirectional plies with the stacking sequence $(0^\circ/60^\circ/0^\circ/-60^\circ/0^\circ/60^\circ/90^\circ/-60^\circ/0^\circ)_s$ representative of the sequence used on launchers' fairing. However, HS rectangular panels of $150 \times 100 \times 3.6$ mm³ are manufactured with 28 unidirectional plies with the stacking sequence $(0^\circ/60^\circ/0^\circ/-60^\circ/0^\circ/60^\circ/90^\circ/90^\circ/-60^\circ/0^\circ/-60^\circ/0^\circ/60^\circ/0^\circ)_s$ in order to have the thickness and the sequence as close as possible to HM panels.

The studied TS is made of "Norcoat Liège" which is natural cork pellets agglomerated by impregnation and polymerisation of a phenolic nitrile resin. Two thermal shield thickness are tested :

- 3.5 mm, typical on launchers' fairing;
- 6.5 mm for analysing the influence of the thermal shield thickness during impact.

Some specimens are presented in figure 2. It can be noticed, that the TS is glued only on the central part of the panels, and not under the clamp system (cf. § II-2), to avoid changing the boundary conditions compared with the unshielded panels.

II-2) Impact test system

The impact test system (cf. figure 3) used to impact the composite coupons is drop weight system. It consists in dropping an impactor, equipped with a load cell, on a 150 x 100 mm² laminate panel, clamped by a 125 x 75 mm² window.

Its principal features are :

- A 2 kg free falling mass ;
- A load cell mounted under the mass to measure the force between the mass and the specimen ;
- An accelerometer mounted over the mass to measure the acceleration. This measure allows to correlate the load cell measure ;
- A spherical impactor of 16 mm diameter ;
- An optical sensor to measure the velocity just before impact ;
- A clamp system to hold the specimen ;
- A control system preventing multiple hits on the specimen ;
- An analogical data acquisition system.

The impact force F_{impact} between the impactor and the specimen is determined due to the measured force, F_{measured} , taken by the load cell:

$$F_{\text{impact}} = \frac{m_{\text{impactor}}}{m_{\text{impactor}} - m_{\text{tip}}} F_{\text{measured}} \quad (1)$$

Where m_{impactor} and m_{tip} are respectively the mass of the impactor and the impactor tip. To determine this expression, the acceleration of the impactor tip and body are of course supposed equal like classiquement admitted in the literature [9]. In this study, the accelerometer signal was not used because it is more noisy than the load cell due to the waves propagation in the impactor [9], but its correlation with the force signal was verified:

$$g_{\text{impact}} = \frac{F_{\text{impact}}}{m_{\text{impactor}}} \quad (2)$$

Where γ_{impact} is the impactor acceleration.

On the figure 4, the impact forces are drawn as a function of time during impact tests on HM panels without and with 6.5 mm TS for different energies. These curves, and all the

other impact ones presented in this article, have been filtered at 15 kHz to avoid a free frequency of the impactor at about 20 kHz. These curves, representative of all performed impact tests, are very classic in the literature [7, 9]. They are globally smooth and almost sinusoidal at low impact energy, with little oscillation due to natural frequencies of the panels. At higher impact energy, they show an important force signal fall followed by oscillations, which is characteristic of delamination onset (from 1.9 J for unshielded panels and 29.4 J for panels with 6.5 mm TS). This result is confirmed by C-scan analyses as well as by others authors [10, 15] in the literature.

Then, due to this load measurement, the projectile tip displacement as a function of time $x(t)$ is obtained by a double integration :

$$x(t) = \int_0^t \left(v_0 + \int_0^t \frac{F_{\text{impact}}}{m_{\text{impactor}}} . dt \right) dt \quad (3)$$

Where v_0 is the initial velocity just before impact.

Afterwards, the impact energy E is evaluated :

$$E = \frac{1}{2} m . v_0^2 \quad (4)$$

II-3) Impact tests results

A lot of impact tests have been performed on HM and HS panels, nude and with 3.5 and 6.5 mm TS (cf. figure 5). We can precise, that to clarify these plots, only a few impact tests on the HM panels have been reported. On these curves, the first impact energy which involves the delamination, measured with C-scan method, is equally reported. These curves show the same force signal peak as soon as the delamination begins. They also show, that with TS, the delamination appears at higher energy and at higher impact force than without TS; cf. figure 6 which plots the energy and the impact force of delamination onset versus the TS thickness.

Therefore, it can be concluded from figure 6, that the TS reveals to be a mechanical protection because it delays the delamination onset. This result is very important for the tolerance damage tolerance concept.

This mechanical protection is, for a part, due to a structure effect of the cork which acts like a spring between the impactor and the composite sheet. This spring stocks a part of the impact energy and thus decreases the maximum force during the impact. This effect is

confirmed by the plot of the maximum impact force versus the impact energy (cf. figure 7) : at low impact energy, the impact force is lower with TS.

But at higher energy the phenomenon is very different; the maximum impact force is higher with TS. This phenomena is also visible on the plot of delaminated area versus the impact energy (cf. figure 8): at low energy the TS protects the composite panel, but at high energy it increases the impact damage area. This behaviour can be attributed to the force spreading effect of the cork which increases the impactor contact area on the composite panel surface. In particular, the maximum impact force, obtained at high energy, near panel perforation, is higher with TS and causes a more extended damage area. A dynamic effect can equally causes this phenomenon, because at high energy the velocities are higher and can cause a modification of the plate deflection mode. However in this study the velocities remains lower than 7 m/s (about 50 J) and the static / dynamic equivalence can be admitted [15]. To separate this force spreading effect of the spring one, the delaminated area versus the impact force has been drawn (cf. figure 9). It can be confirmed that for the same impact force, the delaminated area is lower with TS but the maximum impact force reached is higher and causes more extended damage. The force spreading effect of the TS can be compared to an impactor diameter increasing.

Afterwards, in order to define a damage tolerance demonstration for the shielded panels, the impact depths are measured just after the test and again after 10 days (cf. figure 10). An indentation depth decrease was noted for all specimens. The following reductions were noted:

- 25% on average for unshielded panels ;
- 20 to 25% on average for 3.5 mm TS panels ;
- 10% on average for 6.5 mm TS panels.

Thus, a more important reduction is noted for unshielded composite panels than for shielded ones: the thermal shield acts with less relaxation. Consequently, to cover the time effects (resin viscoelasticity / Norcoat Liege relieving), and in order to be sure to have the expected detectability threshold after few days of storage (0.3 mm according to Airbus certifications), it is necessary to increase the penetration depth of 25% at the moment of the impact. This coefficient does not cover the effects of wet ageing, thermal and fatigue effects. In this study, it is decided to take 0.6 mm of penetration depth as detectability

criterion at the impact's moment, which corresponds to the usual aeronautic criterion called Barely Visible Impact Damage (BVID).

Thus the delaminated area evolution is plotted versus the permanent indentation depth (indentation depth measured after 10 days) (cf. figure 10). The curves show that the composite degradation appears well before having a visible depth on the unshielded composite panels.

Unlike unshielded panels, the mark caused by the impact on the TS is visible before having a delamination in the composite. Therefore, the thermal protection has a shock revealing role and allows detection of impacts before composite delamination onset.

II-4) Materials comparison

It is well known and clearly visible on the materials characteristics (cf. table 1), that the HM material is more brittle than the HS one. In particular, the failure strain in the fibres direction is twice higher for HS than for HM. So, this behaviour is also found in the impact behaviour : the delamination onset energy or impact force is greater for the HS materials (cf. figure 6) and for the same impact energy the delamination area is always larger for the HM panel (cf. figure 8).

Nevertheless the evolutions of the delaminated area versus the impact force or permanent indentation depth are very different for the 2 materials. In fact, when the delamination onset is reached, the delaminated area increases much quicker for the HS material (cf. figure 9 and 10) according to impact force as well as to the permanent indentation. This behaviour is negative for damage tolerance because it will be very difficult to estimate the delamination area in function of the permanent indentation depth, in particular for HS structures.

The reason of this behaviour difference has not yet been explained. On the other hand, complementary works are necessary to understand this phenomenon. In particular, to determine if it is a material effect or another one, like for example stacking sequence or ply thickness...

II-5) Post-impact C-scan and photomicrographs

For impacts that do not result in complete penetration of the target, experiments indicate that damage consists of delaminations, matrix cracking and fibre failures [14]. Investigators have observed that the typical impact damage shape for laminate composites is conical in the thickness direction with the in-plane damage area increase from the impact surface to the backside [16]. Nevertheless, the post-impact C-scan views and the microscope

observations of laminate coupons nude and with TS show three kinds of impact behaviour (cf. figure 11).

For unshielded impacted composite panels, each interface is delaminated (cf. figure 11a). C-scan views show that pairs of twin-triangles develop at each interface. With the rotation of fibres from one ply to the other one, the scheme depicts a typical “double-helix” through the thickness. Increasing from the impacted side to the free side of the plate, delaminations are wrapped in a conical shaped envelope. This result is well-known in the literature [11, 17].

For shielded impacted composite panels and below a certain level of impact energy E_0 (cf. figure 11b), delamination is only located in the middle of the specimen thickness. Matrix cracking are visible in the non-impacted side of the plate. It can be noticed in figure 11b that the photomicrograph represents only a part (20 mm) of the global damage (about 78 mm), and the central delamination only exists outer of this micrograph.

For shielded impacted composite panels and above a certain level of impact energy E_0 (cf. figure 11c), the main delamination is still located in the middle of the coupon thickness, but this delamination is superposed with conic shape delaminations. It can be noticed, like in the previous case, the different images scales.

From these observations, a typical impact damage mode is depicted for each case in the schematic representations shown in the figure 12.

The previously mentioned impact energy threshold E_0 is different for each material and each thermal shield thickness. The different values are given in the table 2 and have been determined by analysing the C-scan views and the photomicrographs.

This very interesting and surprising behaviour is difficult to explain, complementary experimental and numerical investigations will be necessary to deeply understand it. Nevertheless, in our opinion, this different morphology is due to fibres' breakages which appear before the delamination onset in the inferior part of the sample for the shielded panels, and contrary to the unshielded panels where the fibres breakages appear after the delamination onset.

This hypothesis can be confirmed by the numeric calculation of the first fibres breakage during the impact. The panel is classically modelised with composite shell finite elements, and a maximum strain criterion is used. This numeric model shows that the first ply to break is the 60° ply located just above the 0° last ply (non-impacted side), and explains in particular why this breakage is not visible during experiments. This first ply breaks at a

load of 4.2 kN for the HM material and at 5.4 kN for the HS one. These values are reported on the curve of delaminated area versus maximum impact force (cf. figure 9) and show clearly the difference of damage scenario between nude and shielded panels: for nude panels, delamination begins before fibres breakage contrary to the shielded panels case. These broken fibres seem to act like a delamination protection in the inferior part of the panel, perhaps because they decrease the out of plane stresses, delay the delamination onset in this zone and it also begins in the central zone of the panel. This explanation must be confirmed and will be discussed in the paragraph III-3.

II-6) Impact investigation conclusion

Impact experimental investigation allows the following conclusions:

Firstly, the thermal protection has a mechanical protection function: composite damage appears at higher impact energies for shielded laminates, which is favourable for damage tolerance justification. However, above a certain impact energy threshold, delaminated areas reach a saturation point for unshielded panels (composite laminates tend toward perforation), whereas those concerning shielded panels go on increasing. Thus, for impact energies above this threshold, it is possible to have more important delaminated areas for shielded panels than for unshielded ones.

Secondly, the thermal protection has an impact revealing role: the mark caused by the impact on the TS is visible before the composite delamination onsets. However, above a certain indentation depth, delamination area suddenly increases and, for the same indentation depth, the delaminated area for shielded panels is higher than for unshielded ones.

Thirdly, the effect of the TS is globally similar on HS and HM materials; it delays the delamination onset but when the delamination appears, the delaminated area increases very much quicker for the HS material than for HM one.

And finally, the thermal protection modifies the impact behaviour of the composite: the delamination distribution in the laminate thickness changes when specimen are shielded, and the delamination area, which is only the projection of all delaminations in the laminate thickness, is insufficient to characterise the delamination damage in the laminate. This last point seems to be very important because it can allow to test numeric damage model under impact and to improve them due to a test which products different damage morphology than the classical impact on nude panels. This work is actually in progress.

III) Residual strength experimental investigation

III-1) Residual strength test system

As a mean of testing residual strength, compression was chosen because it is among the most critical loading conditions for damaged composite materials and it is reasonably simple to achieve [8, 17]. CAI test setup is shown in figure 13. Anti-buckling knives are used to avoid the global buckling of the sample during the compression. The tested specimens are the two 150 x 100 mm² laminate panels previously mentioned.

The tests were conducted in a 160 kN compression panel testing machine at a displacement rate of 0.2 mm/min. A LVDT sensor was placed at the mid section on the non-impacted side of the specimen to record the out-of-plane displacement. Strain gages were attached at three locations of the coupon (cf. figure 14) :

- face to face, in the middle of the specimens' top. The average of these two strains is a measure of the membrane in-plane loading and the semi-difference is a useful measure of the bending [9].
- On mid-region of the non-impacted side.

Otherwise, two CCD cameras are used to determine the out-of-plane displacement field of the impacted side. The TS is obviously removed before the CAI tests, so the indentation depths are obtained on the carbon and not on the TS.

III-2) Residual strength tests results

In this section, an experimental CAI test on an nude HM panel impacted with 15 J (cf. figure 15) and on a 3.5 mm TS HM panel impacted with 25 J (cf. figure 16) are presented. On the figures 15a and 16a, are plotted the evolution of the 3 strain gages J1', J2 and J2', the compression and flexion strains :

$$\mathbf{e}_{comp} = \frac{J2 + J2'}{2} \quad \text{and} \quad \mathbf{e}_{flex} = \frac{J2 - J2'}{2} \quad (5)$$

On the figures 15c and 16c, the out-of-plane displacement field, measured with 2 CCD cameras, on the impacted side, is drawn for different compression load and for the central part of the sample. The figures 15b and 16b show the sheet deflection, measured by LVDT sensor at the non-impacted side and by the 2 CCD cameras at the impacted side, versus the compression load.

The delamination area measured after the impact tests was respectively 1900 and 4200 mm² for the HM panels nude and with 3.5 mm TS. These delaminated areas, which are

represented on the figure 15c and 16c, are very different in shape. The one of nude panel has a characteristic shape of impact near perforation with two ears induced by the breakage of the last ply, when the one of shielded panel has a circular shape characteristic of low impact energy. The initial indentations are also very different: - 0.53 mm for the nude panel and - 0.15 mm for the shielded one. So even if the delaminated area of the HM nude sample is lower than the shielded one, it is evident that the shielded sample is less damaged than the unshielded one. And in fact, the residual strength of the unshielded sample (160 MPa) is lower than the shielded one (180 MPa).

The CAI test on the unshielded HM panel impacted with 15 J is presented on the figure 15. It can be divided in 3 parts :

- O => A : Compression behaviour :

The test consists globally in compression and the sample's bending is very weak. The local buckle, induced by the impact test, progresses slowly, but already produces an imbalance between the impacted and non-impacted side, which is evident because the J2 gage (impacted side) is lower than the J2' gage (non-impacted side). The deflections of the two sheet sides progress together, so there isn't decohesion in the sheet depth. There are also two little buckles in the positive z direction, near impact mark, appeared during impact test, which progress slowly with the load.

- A => B : Sheet depth increasing :

The panel's behaviour is similar to the previous one, but the deflection of the non-impacted side begins to progress quicker than the impacted one, so there is a decohesion in the sheet depth. But the global bending of the sample remains very weak.

- B => rupture : Final buckling :

The non-impacted side deflection progresses quickly when the impacted side deflection remains constant, and the bending strain increases also quickly, which is characteristic of local buckling behaviour. This local buckling is also visible on the gages' evolution: from the point B, the J2 gage is around constant when the J2' gage increases faster. The two buckles in the positive z direction, near impact mark, increase fast, and initiate the final failure of the sample.

This test is representative of compression on unshielded or shielded panels at high energy; i. e. energy which induces a high permanent indentation. The CAI tests on shielded panels

with weak permanent indentation are different. For example the CAI test on the 3.5 mm shielded HM panel impacted with 25 J is presented figure 16 :

- O => A : Compression behaviour :

The test globally consists in compression and the sample's bending is very weak. The local buckle, induced by the impact test, doesn't progress, but produces yet an imbalance between the impacted and non-impacted side, which is evident because the J2 gage (impacted side) is lower than the J2' gage (non-impacted side).

- A => failure : Final buckling :

The non-impacted side deflection progresses very quickly when the impacted side deflection remains very weak, which is characteristic of buckling behaviour of the non-impacted side. However, the impacted side presents also a buckling in the positive z direction, but above the central buckle. Indeed, the deflection of the central buckle in the negative z direction locks its buckling in this direction. This is this positive buckle which initiate the final breakage.

Therefore, the TS can totally modify the failure scenario of the CAI test, and the residual strength. Furthermore, the delaminated area is not yet a sufficient criterion to estimate the residual strength.

III-3) TS influence on the compression residual strength

At this moment, it is important to study the TS effect on all CAI tests in function of the impact. Figure 17 gives the residual strength evolution versus the impact energy. The reference value of compression failure stress without damage and the theoretical value of buckling failure stress, determined with an analytical approach, are also noted. For the HM panels with 4 simply supported sides, the buckling stress is 320 MPa. Therefore, it is possible to guarantee that the CAI stresses evaluated in this study are not due to global buckling. In fact, the real buckling stress is located between the 4 simply supported sides buckling stress (320 MPa) and the 2 clamped and 2 simply supported sides buckling stress (620 MPa). But for the HS panels, the experiment residual strengths are located between the 4 simply supported sides buckling stress (205 MPa) and the 2 clamped and 2 simply supported sides buckling stress (415 MPa). Moreover, they present an asymptote to about 330 MPa which can be the real buckling stress. So the experimental value of all residual strengths, of HS samples, located near 330 MPa, are not reliable, and must be perhaps situated above this value: this curve (cf. figure 17b) must be used with a lot of precautions.

The three curves of residual strength (cf. figure 17a) for the HM, seem to present an asymptote at the same level towards 145 MPa, which correspond to deformations of about 1600 $\mu\epsilon$. The asymptote corresponds to about 65 % average loss of characteristic in compression relative to an undamaged material ($\epsilon_{I\text{ HM}}^c = 4630 \mu\epsilon$). This result is very important since it shows that, despite a more important saturation delamination area in the case of shielded specimens (cf. figure 8); the maximum diminution of the residual strength is the same than for unshielded specimens. This can probably be justified by the fact that on shielded specimens, the mid-thickness delamination seems to have less influence on the residual strength than the conical shape delaminations obtained on unshielded specimens (because it is less influent on local buckling).

It can be also noted, on the three curves of the HM panels (cf. figure 17a), the residual stress decreases strongly before the delamination appears, in particular for the panels with 6.5 mm TS. This decreasing is due to a different type of damage, which is probably fibres breakage (cf. § II-5). This hypothesis has been confirmed by a numeric model which shows that the first ply to break is the 60° ply located just above the 0° last ply (non-impacted side), and explains in particular why this breakage is not visible during experiments. This first ply breaks at a load of 4.2 kN for the HM material and at 5.4 kN for the HS one (cf. figure 9).

This hypothesis can be also confirmed by the load - displacement curve of the HM panels with 6.5 mm TS obtained at 19.8 J impact (cf. figure 5c). This curve shows, in fact, an inflexion at about 5 mm displacement and 4.5 kN load which is coherent with the first fibre's breakage load found numerically at 4.2 kN.

This phenomenon, of fibres breakage on shielded panels during impact, is more or less observable in impact tests on all shielded panels: at about 4 mm displacement and 4.5 kN load for HM panels with 3.5 mm TS (cf. figure 4b), and 5 mm and 4.5 kN load for HM panels with 6.5 mm TS (cf. figure 4c). It is, in our opinion, a possible explanation of the mid-thickness delamination. In fact, when the fibres breakages propagate in the inferior part of the sheet, shears in this sample part decrease and delay the delamination appearance. So the delamination begins and propagates above this fibres breakage zone, at the middle of the sheet thickness. Complementary works are actually being performed to confirm this conclusion.

The phenomena of the HS panels (cf. figure 17b) are similar to the HM one, but it is more difficult to conclude. At first, the maximum impact energy tested seems insufficient to reach the asymptote for the shielded panels. Nevertheless, the three curves seem to tend to the same asymptote towards 120 MPa, which corresponds to a deformation of about 2400 $\mu\epsilon$. The asymptote corresponds to 80 % average loss of characteristic in compression relative to an undamaged material ($\epsilon_1^c = 12730 \mu\epsilon$). Secondly, the residual strengths are close to real buckling stress, like previously mentioned.

Afterwards, the residual strengths versus delaminated area are plotted (cf. figure 18) for HM and HS panels. The figure for the HM panels (cf. figure 18a) confirms, that for the same delamination area, the mid-thickness delamination obtained on the shielded panels has less influence on the residual strength than the conical shape delamination obtained on unshielded specimens. However, in the same time the residual stress decreases before the delamination appears because of fibres breakages. And like previously, the figure for the HS panels (cf. figure 18b) is more difficult to interpret.

Finally, the residual strength evolution versus the permanent carbon indentation depth is plotted (cf. figure 19). The HM curve (cf. figure 19a) show that the three curves, with or without TS, are relatively similar. This similarity is difficult to explain, but leads to a conclusion that the permanent carbon indentation depth is an important parameter in the characteristic's loss in CAI. And as previously, the figure for the HS panels (cf. figure 18b) is more difficult to interpret, because of the lack of experimental points at high energy.

III-3) Residual strength investigation conclusion

Residual strength experimental investigation allow the following conclusions :

At first, the difference of the damage shape after impact between shielded and unshielded panels is very important on the residual strength. On shielded specimens, the mid-thickness delamination obtained after impact has less influence on the residual strength than the conical shape delaminations obtained on unshielded ones. Hence, for the same delamination area, the residual strength is higher for shielded specimens than for unshielded ones. Nevertheless, the diminution of the residual strength after impact obtained towards the asymptote, i. e. near the sheet perforation, is equivalent for panels with or without TS. In effect the asymptote value is due to the sheet perforation and not to the delamination shape.

Secondly, on shielded specimens, impact damage without delamination, can cause compression characteristic loss. In fact, on shielded panels, fibres breakages start before delamination, contrary to unshielded panels. This original behaviour could allow to test numeric damage model under impact and to improve them by a test which produces different damage chronology than the classical impact on unshielded panels.

Finally, the experimental tests show the permanent carbon indentation seems to be relatively a good indicator to evaluate the residual strength of a shielded or unshielded specimen.

IV) Conclusion

This study attempted to understand the impact and CAI behaviour characteristics in two fibrous composite materials with thermal protection.

Low velocity impact and CAI tests were carried out on shielded and unshielded panels to analyse the thermal protection influence on impacted damaged composite structures used for launchers' fairing.

The TS during the impact test has three main effects:

At first, the thermal protection has an impact revealing role: the mark due to the impact of the thermal shield is well visible before delamination onset. However, above a certain indentation depth, delamination area suddenly increases and it is impossible to estimate the damage size at a given indentation depth.

Secondly, the thermal protection has a mechanical protection function: composite damage appears at higher impact energies for shielded laminates, which is favourable for damage tolerance justification. However, above a certain impact energy threshold, delaminated areas reach a saturation point for unshielded panels (composite laminates tend toward perforation), whereas those concerning shielded panels go on increasing. Thus, for impact energies above this threshold, it is possible to have more important delaminated areas for shielded panels than for unshielded ones.

Finally, the thermal protection modifies the impact behaviour of the composite: the delamination distribution in the laminate thickness changes when specimens are shielded, and the delamination area becomes insufficient to characterise the delamination damage in the laminate.

Two different materials, an HM and an HS one, have been studied, and even if the HM material reveals to be more brittle, the TS influence is similar for the two materials.

Then the TS influence on the CAI tests and particularly on the behaviour modification during the impact has been studied, and leads to the following conclusions:

At first, the TS reveals to be a mechanical protection like during impact: at the same impact energy, the residual strength is higher with TS. But the maximum loss of compression characteristic, reached near perforation is equivalent with or without TS. This behaviour is remarkable because the maximum delaminated area on shielded panels can be twice higher than on unshielded ones. The mid-thickness delamination obtained on shielded panels may have less influence than the conical shape delamination obtained on unshielded specimens. Secondly, this study shows that the delaminated area can't be yet the only criterion to estimate the residual strength, as for the impact on unshielded specimens. And the permanent indentation seems to be an interesting indicator of the residual strength. Finally, a decrease of the residual strength is obtained on shielded panels before the delamination onset. This may be due to fibre breakages appearance before delamination during impact on shielded specimens. This conclusion is very important and must be confirmed by other investigations.

Acknowledgements :

This work was funded by EADS Space Transportation, Saint Médard en Jalles, France. The authors would also like to thank CEAT and the ENSICA's laboratory for their assistance in the post-impact C-scan.

References :

- [1] Rouchon J Certification of large airplane composite structures, recent progress and new trends in compliance philosophy. 7th ICAS congress Stockholm 1990.
- [2] Rouchon J. Fatigue and damage tolerance aspects for composite aircraft structures. Delft 1995.
- [3] Found M.S., Lamb J.R. Impact damage resistance of ring stiffened CFRP panels. *Comp Sci Tech* 2006; 66(2): 215-221.
- [4] Sutherland L.S., Guedes Soares C. Impact behaviour of typical marine composite laminates. *Comp Part B* 2006; 37(2-3): 89-100.
- [5] Sanchez-Saez S., Barbero E., Zaera R., Navarro C. Compression after impact of thin composite laminates. *Comp Sci Tech* 2005, 65(13): 1911-1919.
- [6] Sala G. Post-impact behaviour of aerospace composites for high-temperature applications: experiments and simulations. *Comp Part B* 1997, 28(5-6): 651-665.

- [7] Bull P. H., Edgren F. Compressive strength after impact of CFRP-foam core sandwich panels in marine applications. *Comp Part B* 2004, 35(6-8): 535-541.
- [8] De Freitas M, Reis L. Failure mechanisms on composite specimens subjected to compression after impact. *Comp Str* 1998, 42(4): 365–373.
- [9] Abrate S. *Impact on composite structures*. Cambridge University Press; 1998.
- [10] Guinard S, Allix O, Guedra-DeGeorges D, Vinet A. 3D damage analysis of low velocity low energy impacts on laminated composites by damage mechanics. *Comp Sci Tech* 2002, 62: 585–589.
- [11] Kim RY, Soni SR Experimental, analytical studies on the onset of delamination in laminated composites. *J Comp Mat* 1984, 18: 70–80.
- [12] Coutellier D., Walrick J.C., Geoffroy P. Presentation of a methodology for delamination detection within laminated structures. *Comp Sci Tech* 2006, 66(6): 837-845.
- [13] KHONDKER O.A., KERSZBERG I., HAMADA H. Measurements and prediction of the compression-after-impact strength of glass knitted textile composites. *Comp Part A* 2004, 235 : 145-157.
- [14] ZHOU G. Compressive behaviour of large undamaged and damaged thick laminated panels. *Comp Str* 1997, 38: 589-597.
- [15] Kwon Y. S., Sankar B. V. Indentation flexure and low velocity impact damage in graphite epoxy laminate. *J Comp Tech Res* 1993, 15(2): 101-111.
- [16] FIN S.R., SPRINGER G.S. Delaminations in composite plates under transverse static or impact loads – experimental results. *Comp str* 1993, 23 : 191-204.
- [17] KHONDKER O.A., KERSZBERG I., HAMADA H. Measurements and prediction of the compression-after-impact strength of glass knitted textile composites *Comp Part A* 2004, 35: 145-157.
- [18] DE FREITAS M., REIS L. Failure mechanisms on composite specimens subjected to compression after impact. *Comp Str* 1998, 42: 365-373, 1998.

Figures Caption :

Figure 1 : Characterisation of the effect of accidental damage

Figure 2 : Specimens without (a) and with (b) TS

Figure 3 : Impact apparatus

Figure 4 : Experimental impact force during impact tests on HM panels without (a) and with 6.5 mm (b) TS

Figure 5 : Load – displacement curves for HM impact tests without TS (a), with 3.5 mm (b) and 6.5 mm (c) TS at different impact energies

Figure 6 : Energy (a) and impact force (b) of delamination onset for HM and HS panels versus the TS thickness

Figure 8 : Delaminated area versus impact energy for HM (a) and HS (b) panels

Figure 9 : Delaminated area versus maximum impact force for HM (a) and HS (b) panels

Figure 10 : Delaminated area versus permanent indentation depth for HM (a) and HS (b) panels

Figure 11 : Post-impact C-scan and photomicrographs on HS panels

Figure 12 : Typical impact damage mode of composite panels without TS (a) , with TS for $E < E_0$ (b), and with TS for $E > E_0$ (c).

Figure 13 : CAI apparatus

Figure 14 : Strain gages location on the coupon

Figure 15 : CAI of unshielded HM panel impacted with 15 J : Strain evolution (a), deflection (b), and out of plane displacement field (c)

Figure 16 : CAI of HM panel with 3.5 mm TS impacted with 25 J : Strain evolution (a), deflection (b), and out of plane displacement field (c).

Figure 17: Residual strength versus impact energy for HM (a) and HS (b) panels

Figure 18: Residual strength versus delaminated area for HM (a) and HS (b) panels

Figure 19 Residual strength versus permanent carbon indentation for HM and HS panels

Tables :

	HM	HS
E_1^t (GPa)	230	130
E_1^c (GPa)	190	110
E_2 (GPa)	4.6	8.4
G_{12} (GPa)	3.8	4.8
σ_1^t (MPa)	1300	1500
σ_1^c (MPa)	880	1400
σ_2^t (MPa)	26	35
σ_2^c (MPa)	120	120
τ_{12} (MPa)	74	100
ϵ_1^t ($\mu\epsilon$)	5650	11540
ϵ_1^c ($\mu\epsilon$)	4630	12730
Ply thickness (mm)	0.21	0.13
ν_{12}	0.27	0.35

Table 1 : Mechanics characteristic of the HM and HS materials

E_0 values (J)	3.5 mm TS	6.5 mm TS
HM	20	> 25
HS	30	35

Table 2 : E_0 values for HM and HS panels

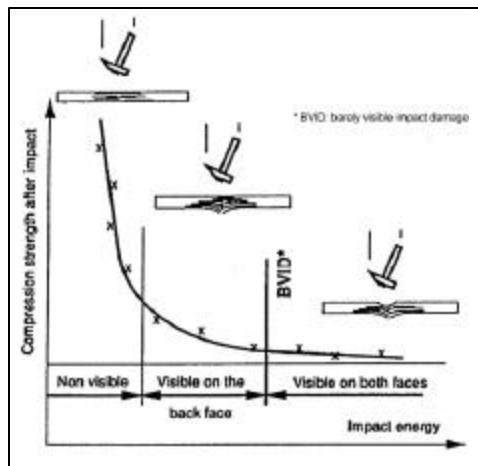


Figure 1 : Characterisation of the effect of accidental damage

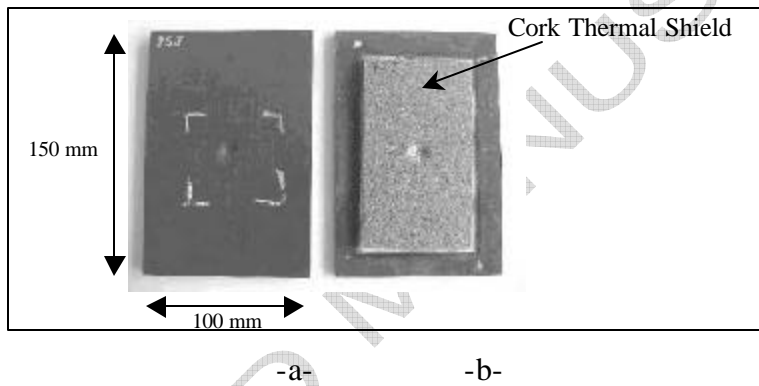


Figure 2 : Specimens without (a) and with (b) TS

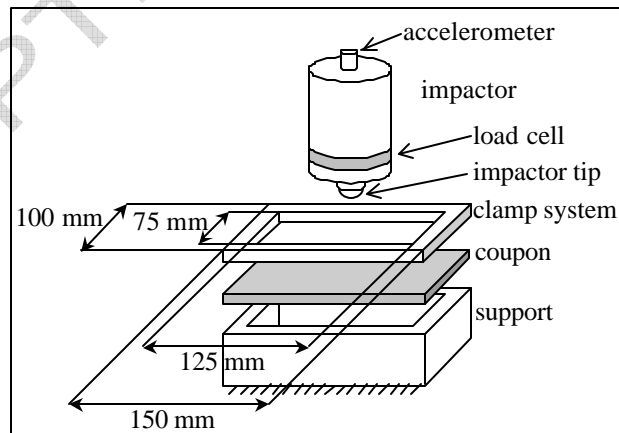


Figure 3 : Impact apparatus

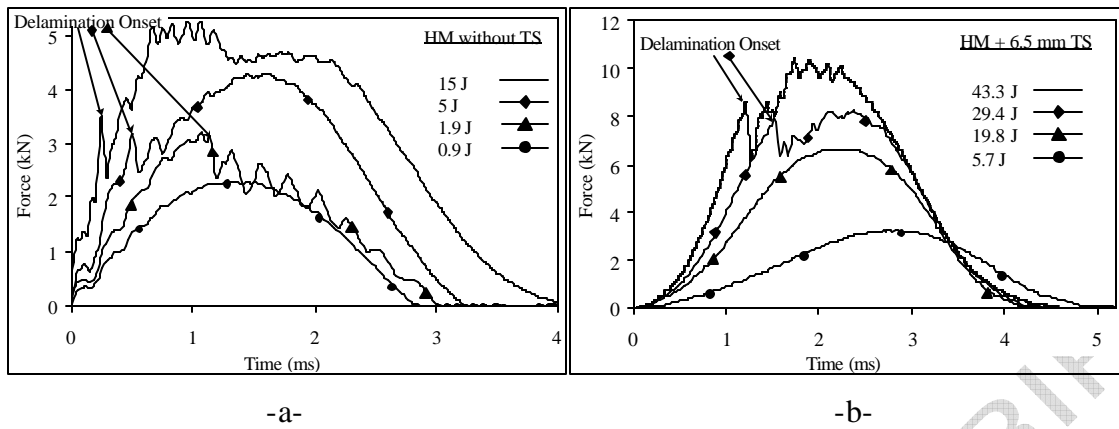


Figure 4 : Experimental impact force during impact tests on HM panels without (a) and with 6.5 mm (b) TS

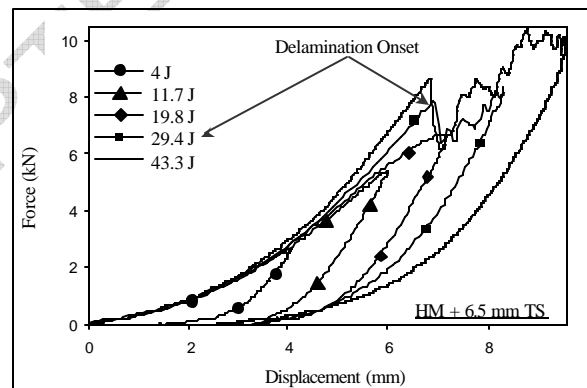
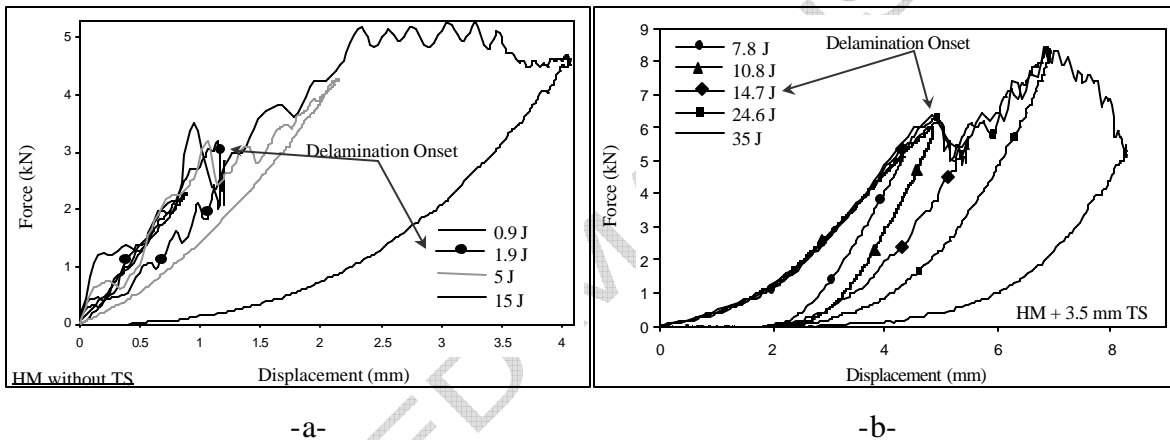
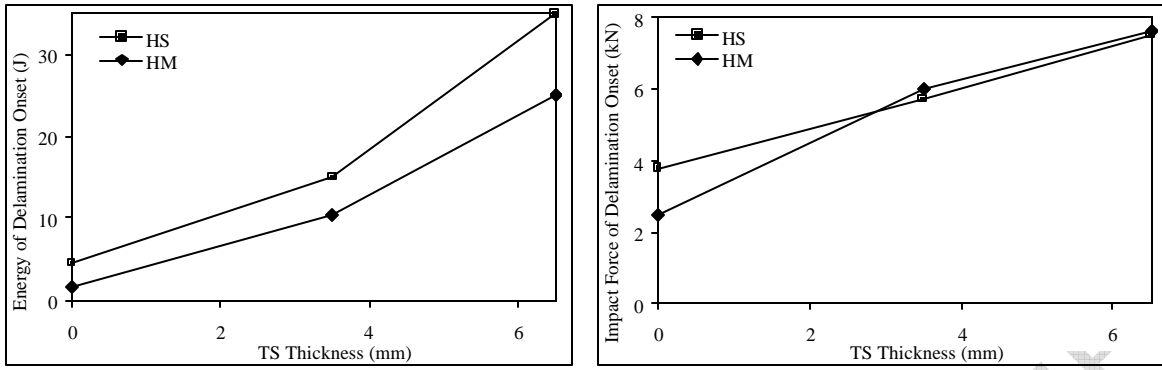


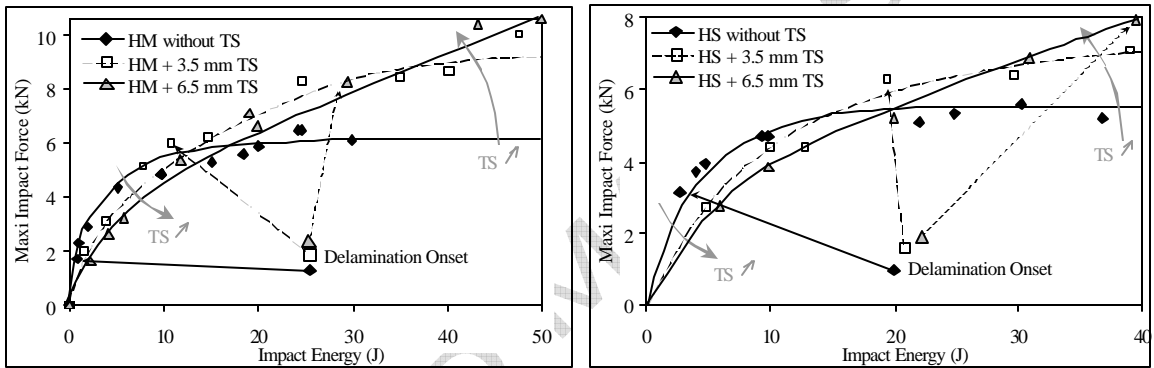
Figure 5 : Load – displacement curves for HM impact tests without TS (a), with 3.5 mm (b) and 6.5 mm (c) TS at different impact energies



-a-

-b-

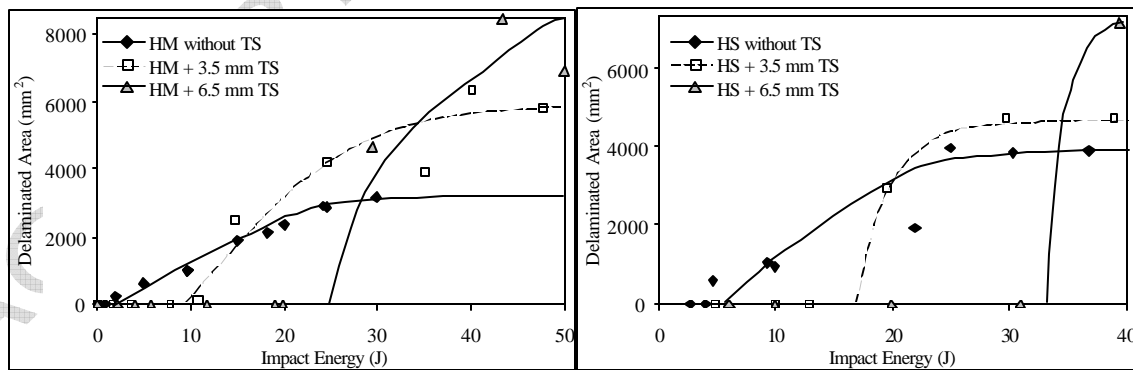
Figure 6 : Energy (a) and impact force (b) of delamination onset for HM and HS panels versus the TS thickness



-a-

-b-

Figure 7 : Maximum impact force versus impact energy for HM (a) and HS (b) panels



-a-

-b-

Figure 8 : Delaminated area versus impact energy for HM (a) and HS (b) panels

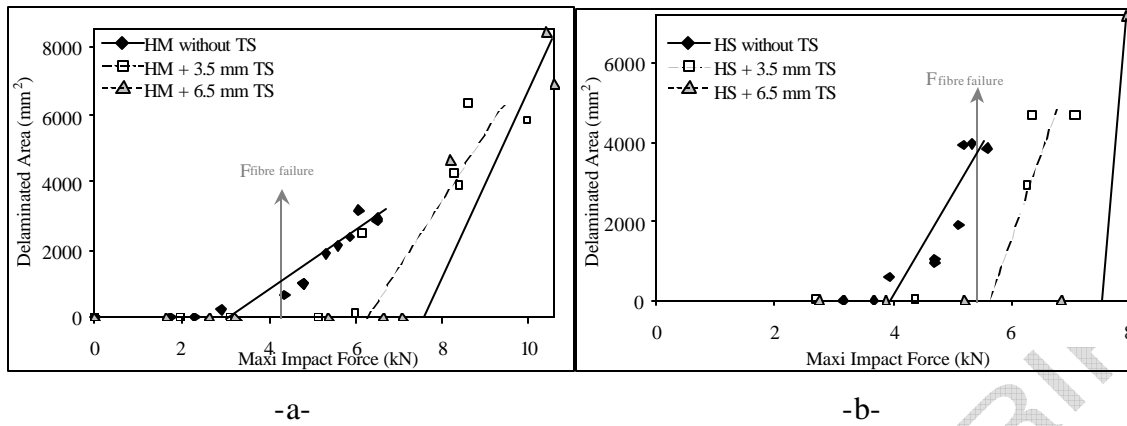


Figure 9 : Delaminated area versus maximum impact force for HM (a) and HS (b) panels

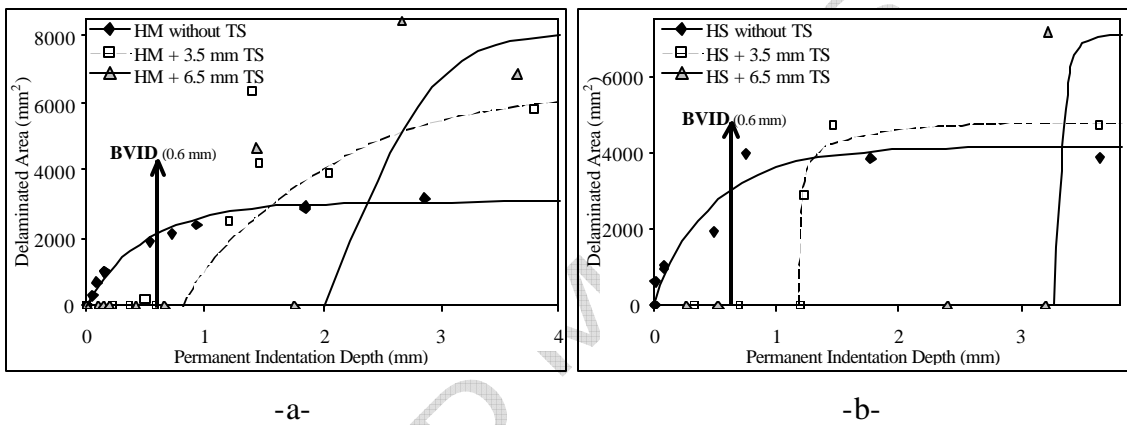
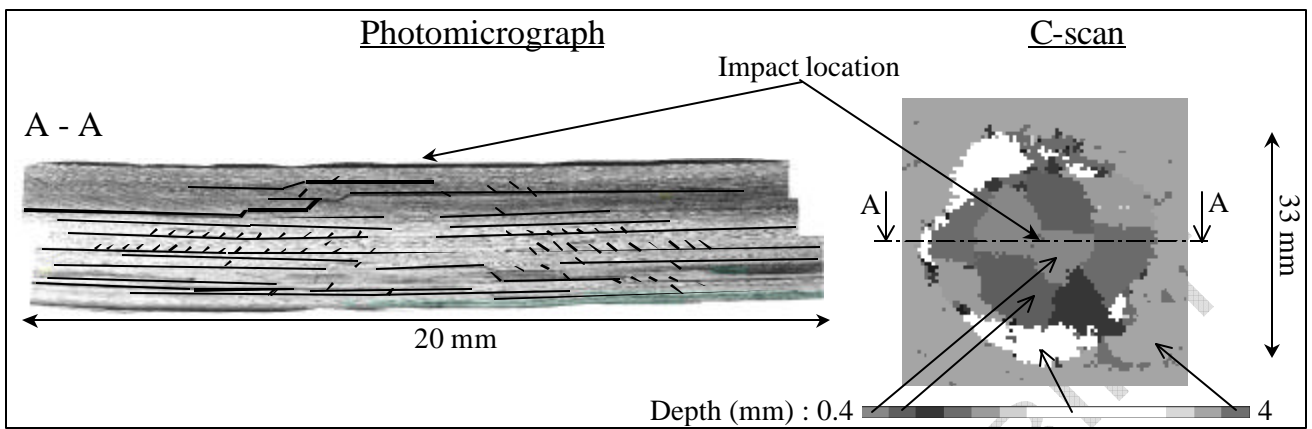
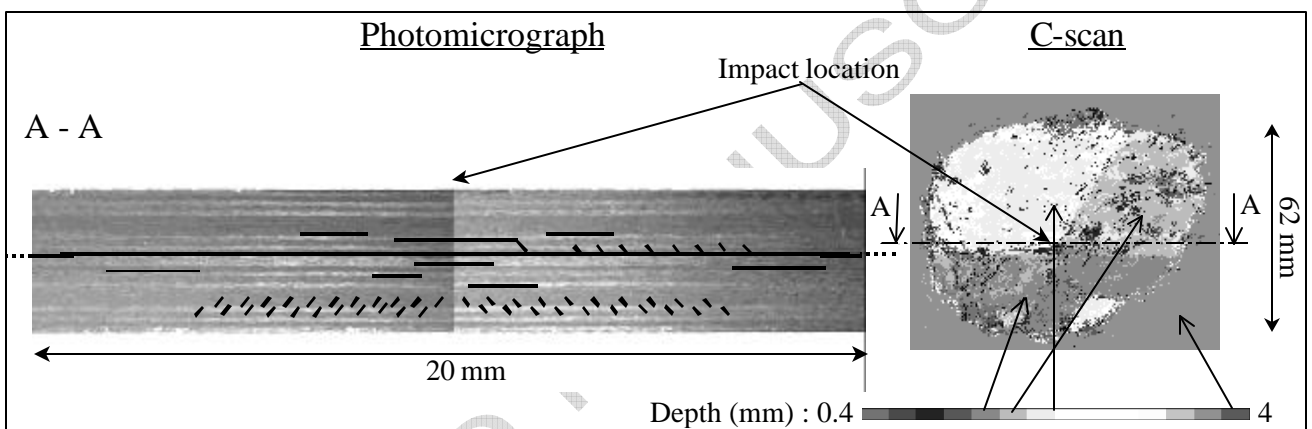


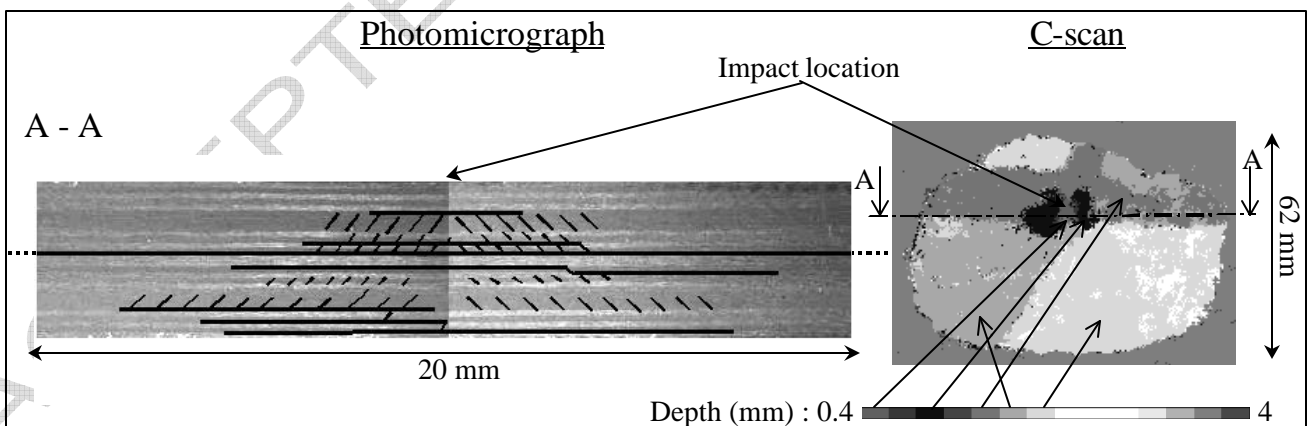
Figure 10 : Delaminated area versus permanent indentation depth for HM (a) and HS (b) panels



-a- : Unshielded HS panel impacted with 7 J



-b- : 3.5 mm HS panel impacted with 20 J



-c- : 6.5 mm HS panel impacted with 30 J

Figure 11 : Post-impact C-scan and photomicrographs on HS panels

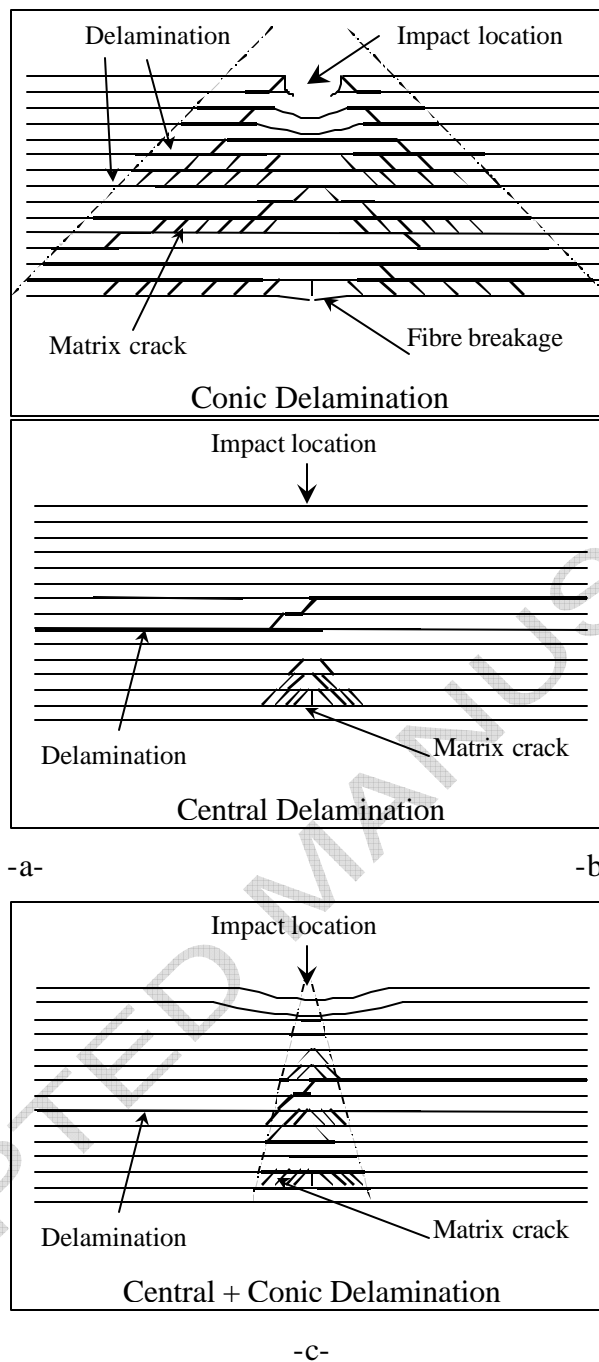


Figure 12 : Typical impact damage mode of composite panels without TS (a) , with TS for $E < E_0$ (b), and with TS for $E > E_0$ (c).

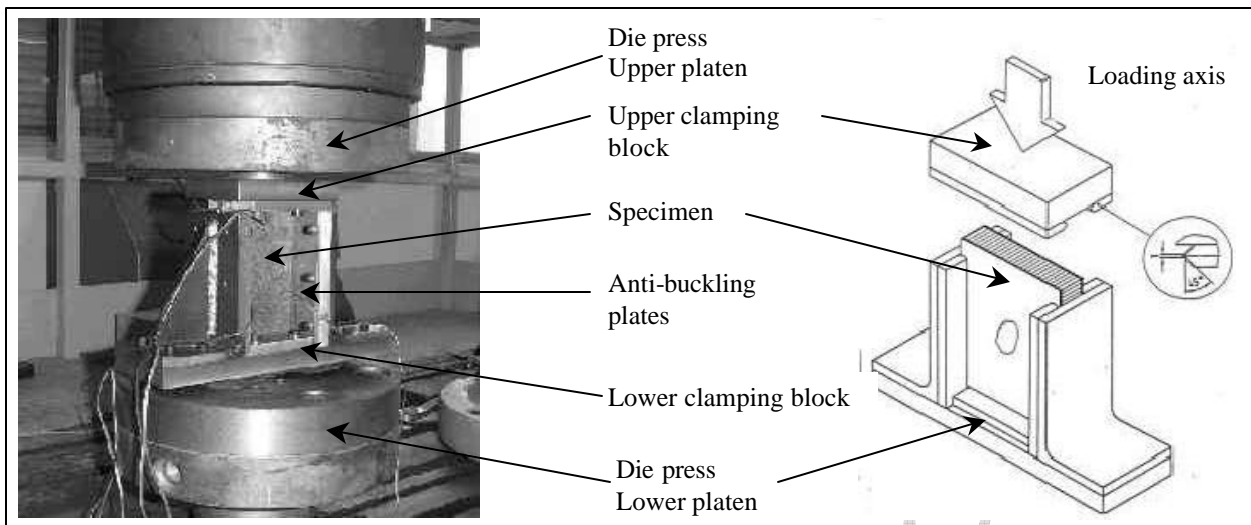


Figure 13 : CAI apparatus

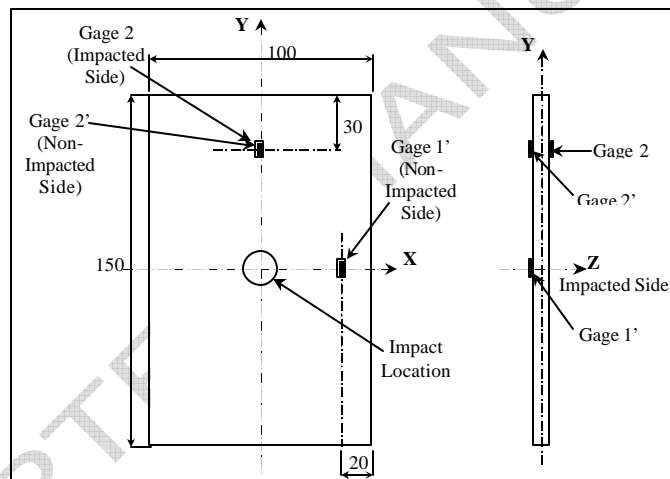
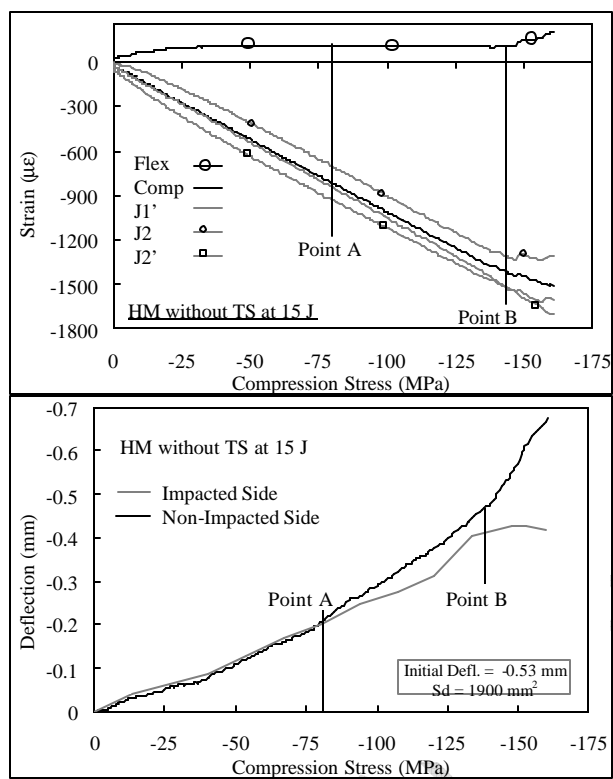
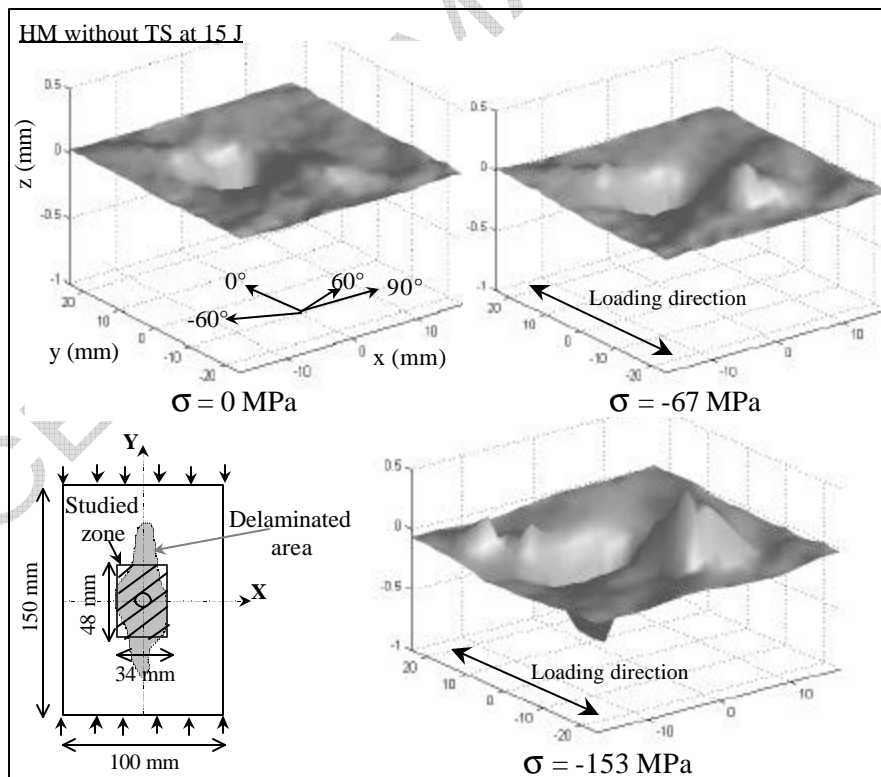


Figure 14 : Strain gages location on the coupon



-a-

-b-



-c-

Figure 15 : CAI of unshielded HM panel impacted with 15 J : Strain evolution (a), deflection (b), and out of plane displacement field (c)

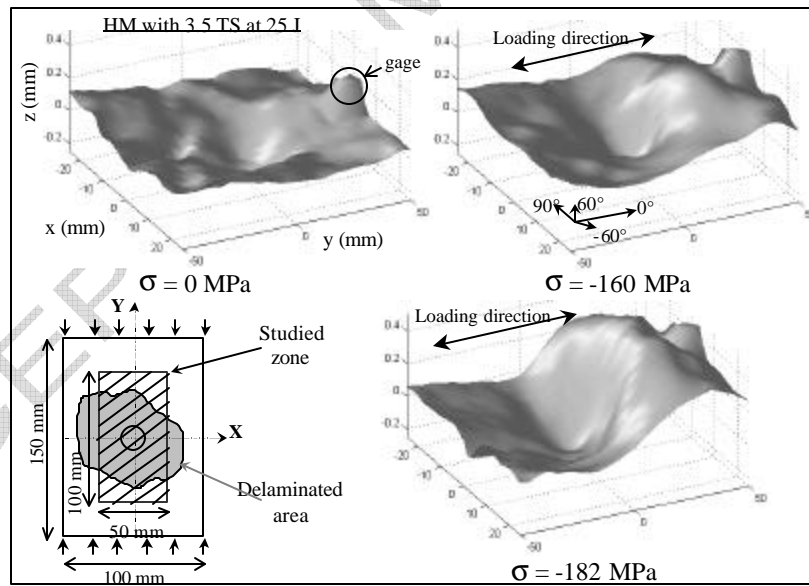
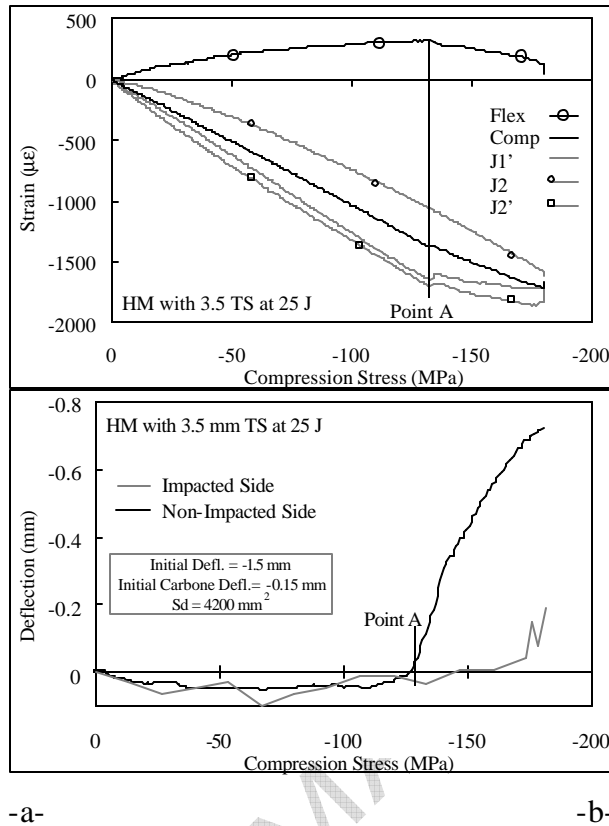


Figure 16 : CAI of HM panel with 3.5 mm TS impacted with 25 J : Strain evolution (a), deflection (b), and out of plane displacement field (c).

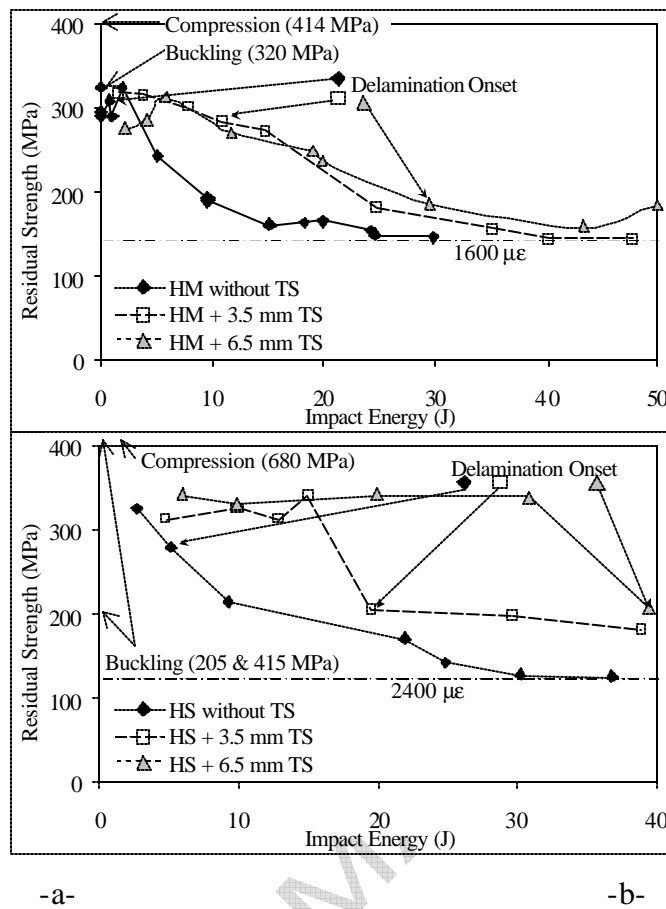


Figure 17: Residual strength versus impact energy for HM (a) and HS (b) panels

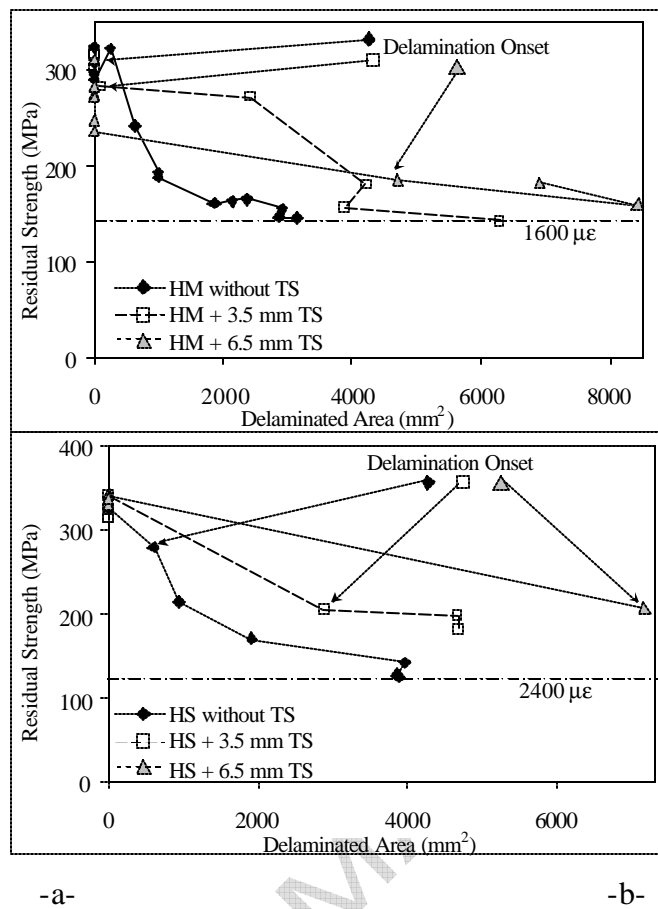


Figure 18: Residual strength versus delaminated area for HM (a) and HS (b) panels

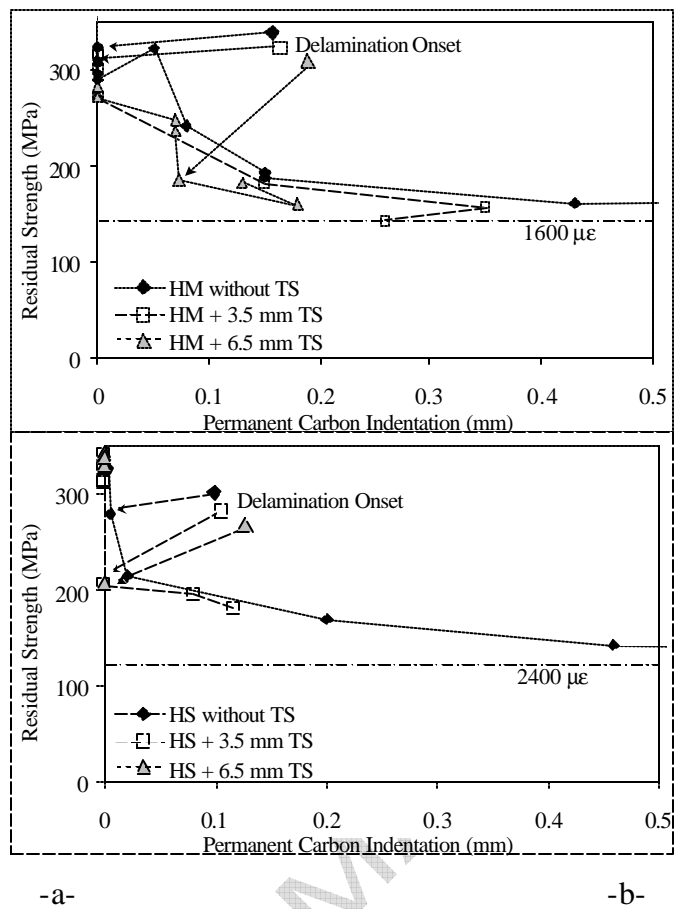


Figure 19 Residual strength versus permanent carbon indentation for HM and HS panels